Kinetic and Thermodynamic Conformational Polymorphs of Bis(p -tolyl) Ketone p -Tosylhydrazone: The Curtin−Hammett Principle in Crystallization

ARTICLE *in* CRYSTAL GROWTH & DESIGN · AUGUST 2007

Impact Factor: 4.89 · DOI: 10.1021/cg070542t

2 AUTHORS:

Saikat Roy
Tata Chemicals Ltd.
18 PUBLICATIONS **294** CITATIONS
SEE PROFILE

Ashwini Nangia
University of Hyderabad
273 PUBLICATIONS **7,114** CITATIONS
SEE PROFILE

CRYSTAL GROWTH & DESIGN
2007
VOL. 7, NO. 10
2047−2058

Kinetic and Thermodynamic Conformational Polymorphs of Bis(*p*-tolyl) Ketone *p*-Tosylhydrazone: The Curtin−Hammett Principle in Crystallization

Saikat Roy and Ashwini Nangia*

School of Chemistry, University of Hyderabad, Hyderabad 500 046, India

Received June 15, 2007; Revised Manuscript Received July 4, 2007

ABSTRACT: Bis(*p*-tolyl) ketone *p*-tosylhydrazone (**2**) crystallized as three conformational polymorphs, forms 1−3, under different conditions. The crystal structure of form 1 has an N−H···O═S dimer synthon, but forms 2 and 3 have no strong hydrogen bonds even though the molecule contains an SO_2NH group. Polymorphs 1 and 3 are assigned as kinetic and thermodynamic forms on the basis of the criteria of lower energy, higher melting point, and higher density for the latter modification. Calculation of both intramolecular (E_{conf}) and intermolecular energy (U_{latt}) gave a crystal energy difference (ΔE_{total}) of 2.54 kcal mol^{-1} between forms 1 and 3, whereas metastable and disappearing form 2 has much a higher energy of 8.71 kcal mol^{-1}. Sulfonamide **2** is a rare example of a polymorph cluster wherein strong hydrogen bonds stabilize kinetic form 1 whereas thermodynamic polymorph 2 has excellent close packing but no hydrogen bonds. A Curtin−Hammett energy profile for the crystallization of conformational polymorphs 1 and 3 is proposed that is consistent with structural, thermochemical, and computational data. Hydrogen bonding in tolyl compound **2** is compared with other benzophenone hydrazones varying at the *para*-position (e.g., H, F, Cl, Br). The bimolecular N−H···O═S dimer is present in crystal structures **3**−**6** as well as in the CH_2Cl_2 solvate of **2** and benzene solvates of chloro **5** and bromo **6** hydrazones.

Introduction

Polymorphism is the existence of the same chemical compound in more than one crystalline modification in the solid state.[1] After more than a century of research[2] on this historically enigmatic and now pharmaceutically important phenomenon, a proper understanding of how crystallization occurs and why certain compounds are polymorphic is still not clear. Several factors influence the crystallization of polymorphs, such as solvent, temperature, additives, and cocrystal formers.[3] McCrone's forecast[1a] "that the number of forms known for a given compound is proportional to the time and money spent in research on that compound" appears prophetic today. Crystal structures of a second polymorph of aspirin,[3e] benzamide,[3d] and maleic acid,[3h] two polymorphs of methacrylamide,[3i] a third form of venlafaxine hydrochloride,[3m] four polymorphs of benzidine,[3j] and four new forms of oxalyl dihydrazide[3k] were reported recently.

Kitaigorodskii[4] stated that molecular crystals are organized in the most efficient use of space, such that bumps fit into hollows, with an average packing coefficient of 0.72 for aromatic and hydrocarbon-like molecules (typical range 0.65−0.77 for organic crystals). Etter[5] postulated hydrogen-bonding rules, and Desiraju[6] advocates supramolecular synthons to understand how molecules organize via energetically favored patterns of hydrogen bonds and robust synthons.[7] Whenever hydrogen-bonding functional groups are available in a molecule, they are used in molecular recognition and self-assembly for crystallization.[8] The lack of or incomplete use of H bond donors/acceptors in a crystal structure attracted special mention.[9]

Recent papers[10] suggest the following model of crystallization for polymorphs: the kinetic crystal nucleates faster via a lower activation energy pathway compared to the thermodynamic form which is more stable but it should cross over a higher energy barrier. Naturally, if the kinetically favored form is also more stable then polymorphism is unlikely. Desiraju[11] likened crystallization to a supramolecular reaction leading to kinetic and thermodynamic products (polymorphs) through Curtin−Hammett like reaction kinetics. Are there examples of molecules containing H-bonding functional groups that crystallize in a hydrogen-bonded form (kinetic) and another close-packed, dense polymorph (stable)? Such crystal structures would be ideal test cases to understand kinetic−thermodynamic factors in polymorph crystallization.[12] Polymorphs that differ in the nature of H bond synthon or molecular conformation or overall packing features are well documented,[3] but it is quite rare to find a hydrogen-bonded crystal structure and another close-packed polymorph without strong H bonds. This paper deals with crystal structures in the latter uncommon category.

Results and Discussion

A search of the Cambridge Structural Database[13] showed that there are 93 crystal structures in the "polymorph/form/modification/morph" category that contain OH/NH groups but these donors are not used in H bonding, either due to steric congestion or because of a less electronegative acceptor (see Table S1 for CSD refcodes). Of these 93 structures, a second polymorph with conventional H bonds was found in only four cases (Scheme 1)—KUVWON,[14a] MAMGUD,[14b,c] UCUGOP,[14d] and WEFKEY.[14e] There are two examples of an O−H···O or N−H···N hydrogen bond in one structure compared to weaker O−H···π[14a] or N−H···π[14d] interaction in another form, whereas in two remaining cases O−H···N/N−H···O H bond is present in one structure but absent in the second form.[14b,c,e] These latter two examples were reported during the course of our experiments, but kinetic/thermodynamic and crystal lattice energy relations of H-bonded vs non-H-bonded polymorphs were not discussed. Price and co-workers[15] computationally studied alloxan, an archetype amide with no conventional N−H···O hydrogen bonds in its crystal structure. Even though computer-predicted hydrogen-bonded forms of alloxan lie in the energy range for polymorphs (about 10 frames within 1 kcal mol^{-1}), no experi-

* To whom correspondence should be addressed. Fax: +91 40 2301 1338. E-mail: ashwini_nangia@rediffmail.com.

10.1021/cg070542t CCC: $37.00
Published on Web 08/18/2007

Scheme 1. Four Polymorph Pairs in the CSD in Which There Is Strong H Bonding in One Crystal Structure and Weaker or No H Bonding in the Other Form, As Indicated against Their Refcodes[a]

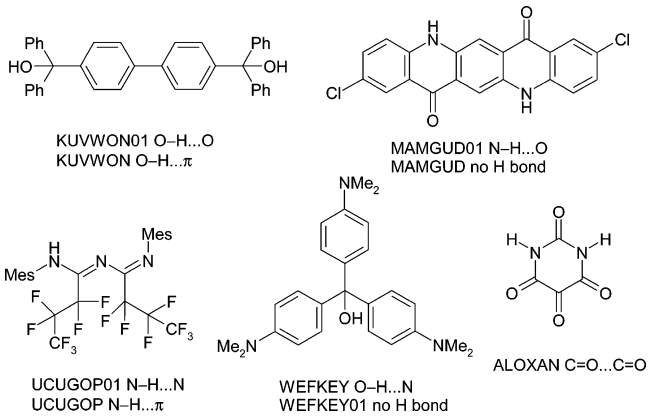

[a] The crystal structure of alloxan is stabilized by dipolar interactions, but its H-bonded form is not known.

Scheme 2. (a) Phenylogue Series in Polymorph Clusters,[18] (b) from Dimorphs of Acetone Tosylhydrazone 1 → Trimorphs of Tolyl Tosylhydrazone 2 (This Paper) by Phenyl Extension, and (c) Derivatives 3−7 Analyzed for Polymorphism

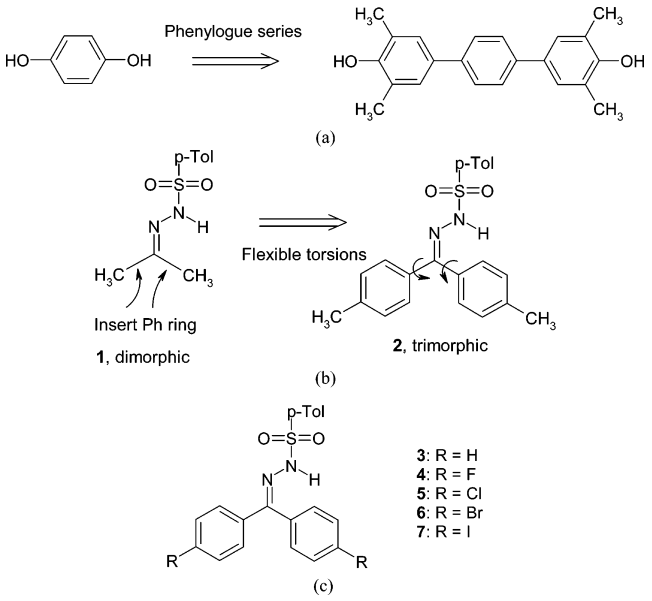

mental H-bonded polymorph of alloxan is known. In the above background, we report the title polymorphic system **2** wherein an N−H···O═S hydrogen bond dimer is present in the crystal structure of form 1, whereas form 3 is stabilized by close packing to the exclusion of H bonds. The classification of polymorphs in H-bonded or non-H-bonded category is based on strong, conventional H bonds, i.e., O−H···O, N−H···O, and O−H···N with energy of 5−10 kcal mol^{-1}.[16] Weaker C−H···O and N−H···π interactions are discussed in the crystal structure analysis.

Bis(*p*-tolyl) ketone *p*-tosylhydrazone (**2**) (Scheme 2) was taken up for polymorphism studies for the following reasons. (1) It contains the pharmaceutically important SO_2NH group. (2) The molecular structure can be independently varied at Ar−SO_2 and Ar−C−Ar portions to give several closely related analogues. (3) Acetone tosylhydrazone (**1**) exhibits conformational dimorphism.[17] The last point suggested a molecular engineering approach to polymorph clusters. For example,

Scheme 3. Occurrence Probability of Hydrogen Bond Motifs of the Sulfonamide Group in a Subdatabase of 1266 Crystal Structures (CSD)

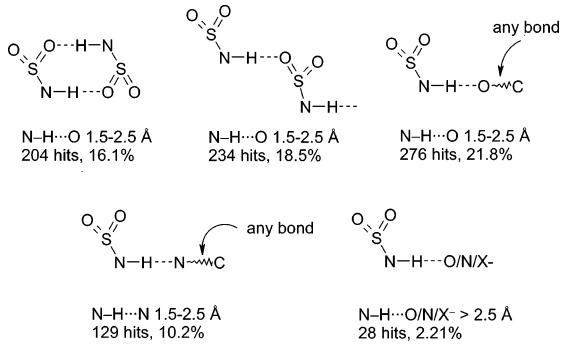

hydroquinone and 4,4′-terphenyldiol make a phenylogue-extended series of polymorphs,[18] leading to the thought that acetone and tolyl ketone hydrazones **1** and **2** may give another phenylogue-related polymorph cluster. Similarity in hydrogen bonding and packing motifs of closely related molecules (e.g., homologues, cis−trans isomers, stereoisomers, cycloalkene/cycloalkane analogs) is termed morphotropism.[19] However, phenyl extension of molecular structure leading to polymorphism and isostructurality is not studied, except one example.[18] Interestingly, molecule **2** afforded three polymorphs in the following sequence: it crystallized as form 1 (space group *C*2/*c*) having an SO_2NH···O═S dimer and two additional polymorphs (forms 2 and 3 in space group *C*2/*c* and *P*2$_1$/*c*) wherein the NH donor surprisingly does not engage in N−H···O hydrogen bonds with the SO_2 acceptor.

The sulfonamide functional group is present in sulfa drugs which have a high propensity for polymorphism (ca. 50%) and pseudopolymorphism (over 100 solvates of sulfathiazole).[3f,20] Two self-complementary hydrogen bond synthons of the SO_2NH group are bimolecular dimer and extended catemer of graph set notation $R_2^2(8)$ and $C(4)$.[21] The occurrence probability[7a] of dimer and catemer synthons was estimated as 16.1% and 18.5% (Scheme 3) among 1266 accurately determined organic sulfonamide hits in the CSD.[13] Polymorphism in sulfonamides typically involves the NH donor approaching the S═O group or another competing acceptor, such as carbonyl C═O, ether/alcohol C−O, or pyridine N. Alternatively, molecules may be assembled via the same H bond synthon but they exist in different conformations. These situations are classified as synthon polymorphism[10a] (different H bond motifs), conformational polymorphism[22] (different conformations in different structures), and packing polymorphism[10d] (differences in crystal packing but similar conformation/synthon). There is no example of polymorphic sulfonamides that differ by the presence of N−H···O/N hydrogen bonds in one crystal structure and absence of H bonding in another form.

Conformational Polymorphs of 2. Crystallization of **2** from EtOH/CH_2Cl_2 afforded single crystals for X-ray diffraction. Structure solution and refinement in *C*2/*c* space group (Table 1) showed the expected SO_2NH dimer synthon (N−H···O: 1.99 Å, 159°, Table 2). The phenyl CH donors connect molecular aggregates (Figure 1) via C−H···O and C−H···π interactions (2.45, 2.53 Å). Solvent-drop grinding (or kneading) is a recent method in polymorph screens[23] because of its good success rate in giving new polymorphs. Grinding **2** with a few drops of CH_2Cl_2 and using the microcrystalline powder as seed afforded single crystals of form 2 in *C*2/*c* space group. We obtained twinned crystals despite several attempts, and the best of these was mounted on the goniometer for X-ray data collection.

Table 1. Crystal Data for Sulfonamides 2−6

param	**2** (R = Me) form 1	**2** (R = Me)[a] form 1	**2** (R = Me) form 2	**2** (R = Me) form 3
empirical formula	$C_{22}H_{22}N_2O_2S$	$C_{22}H_{22}N_2O_2S$	$C_{22}H_{22}N_2O_2S$	$C_{22}H_{22}N_2O_2S$
fw	378.48	378.48	378.48	378.48
cryst syst	monoclinic	monoclinic	monoclinic	monoclinic
space group	*C*2/*c*	*C*2/*c*	*C*2/*c*	$P2_1/c$
T (K)	100(2)	298(2)	298(2)	298(2)
a (Å)	22.0093(13)	22.250(3)	42.043(8)	8.2971(5)
b (Å)	11.9763(7)	12.1201(15)	8.0381(16)	39.758(3)
c (Å)	15.1853(9)	15.2891(19)	12.345(3)	5.9349(4)
α (deg)	90	90	90	90
β (deg)	100.937(1)	100.538(2)	104.08(3)	97.2940(10)
γ (deg)	90	90	90	90
Z	8	8	8	4
V (Å^3)	3930.0(4)	4053.5(9)	4046.5(14)	1942.0(2)
D_{calcd} (g cm^{-3})	1.279	1.240	1.242	1.295
R_1 ($I > 2\sigma(I)$)	0.0408	0.0501	0.0724	0.0464
wR_2	0.1047	0.1307	0.1405	0.1128
S	1.072	1.037	0.950	1.135

param	**2**·0.5CH_2Cl_2	**3** (R = H)	**4** (R = F)	**5** (R = Cl)
empirical formula	$C_{22}H_{22}N_2O_2S{\cdot}0.5CH_2Cl_2$	$C_{20}H_{18}N_2O_2S$	$C_{20}H_{16}F_2N_2O_2S$	$C_{20}H_{16}Cl_2N_2O_2S$
fw	420.94	350.42	386.41	419.31
cryst syst	triclinic	monoclinic	monoclinic	monoclinic
space group	$P\bar{1}$	$P\bar{1}$	$P2_1/c$	*C*2/*c*
T (K)	100(2)	298(2)	298(2)	100(2)
a (Å)	7.9174(18)	9.8402(16)	12.3523(16)	22.4996(17)
b (Å)	11.701(3)	10.1297(16)	9.2366(12)	11.4602(7)
c (Å)	13.248(3)	10.5669(17)	16.492(2)	15.4310(9)
α (deg)	111.862(4)	117.517(2)	90	90
β (deg)	107.198(4)	95.800(2)	103.942(2)	102.552(2)
γ (deg)	93.619(4)	99.945(2)	90	90
Z	2	2	4	8
V (Å^3)	1067.1(4)	900.2(3)	1826.2(4)	3883.8(4)
D_{calcd} (g cm^{-3})	1.310	1.293	1.405	1.434
R_1 ($I > 2\sigma(I)$)	0.0579	0.0524	0.0334	0.0317
wR_2	0.1385	0.1320	0.0855	0.0833
S	1.028	1.030	1.048	1.057

param	**5**·0.5PhH	**6** (R = Br)	**6**·0.5PhH
empirical formula	$C_{20}H_{16}Cl_2N_2O_2S{\cdot}0.5C_6H_6$	$C_{20}H_{16}Br_2N_2O_2S$	$C_{20}H_{16}Br_2N_2O_2S{\cdot}0.5C_6H_6$
fw	458.36	508.23	547.28
cryst syst	triclinic	orthorhombic	triclinic
space group	$P\bar{1}$	*Pbca*	$P\bar{1}$
T (K)	298(2)	100(2)	298(2)
a (Å)	7.9816(16)	11.4666(7)	8.0184(8)
b (Å)	11.793(2)	15.5694(9)	11.9872(12)
c (Å)	13.501(3)	22.2113(13)	13.5855(13)
α (deg)	112.409(3)	90.00	112.826(2)
β (deg)	106.616(3)	90.00	106.592(2)
γ (deg)	93.815(3)	90.00	93.964(2)
Z	2	8	2
V (Å^3)	1103.5(4)	3965.3(4)	1129.26(19)
D_{calcd}/g cm^{-3}	1.380	1.703	1.610
R_1 ($I > 2\sigma(I)$)	0.0418	0.0241	0.0391
wR_2	0.1080	0.0589	0.0899
S	1.023	1.031	1.030

[a] The crystal structure of form 1, compound **2**, was redetermined at 298 K for direct comparison of packing coefficient and crystal density with forms 2 and 3.

Crystal structure solution (using CELL_NOW and TWINABS; see Experimental Section) showed an unexpected result. The strong NH donor is not involved in H bonding up to H···O < 3.0 Å, but SO_2 acceptors are connected to CH donors in normal C−H···O interactions of <2.7 Å. A third modification, form 3, was discovered upon crystallizing compound **2** from EtOH ($P2_1/c$ space group). Once again, the sulfonamide NH donor does not engage in N−H···O bond or N−H···π interaction. There is a two-point C−H···O motif from phenyl CH donors to SO_2 group (∼2.5 Å), but there are no short contacts between molecules aligned along the monoclinic *b*-axis (=39.76 Å). Crystal forms 2 and 3 have similar molecular packing in the monoclinic crystal system, but both structures are devoid of N−H···O bonds (Figures 2 and 3). C−H···O interactions are identified in all three forms (Table 2). Density and packing fraction of the H-bonded structure 1 is lower than form 2, and form 3 has the highest crystal density (packing fraction 64.6, 64.7, 67.9%; density 1.240, 1.242, 1.295 g cm^{-3}). The tolyl rings are better eclipsed and consequently more efficiently close-packed in crystal form 3 compared to 2 (Figure 4). There is one symmetry-independent molecule in the unit cell of each polymorph, but the flexible molecule adopts a different conformation in each crystal structure; i.e., forms 1−3 are conformational polymorphs (Figure 5).

The bulk purity of polymorphic solids 1 and 3 was judged to be good by comparison of their experimental powder X-ray diffraction pattern with that calculated from the X-ray structure (Figure S1). After isolation of form 3, we were unable to recover

Table 2. Hydrogen Bond Geometry in Sulfonamide Crystal Structures 2−6[a]

compd	interaction	d(H···A) (Å)	D(D···A) (Å)	θ(∠D−H···A) (deg)	τ_1(N2−N1−S1−C5) (deg)
2, form 1 (100 K)	N(1)−H(1)···O(1)	1.99	2.954(2)	159	65.9
	C(11)−H(11)···O(2)	2.44	3.520(2)	173	
	C(16)−H(16)···O(2)	2.45	3.205(2)	126	
	C(6)−H(6)···O(2)(intra)	2.47	2.886(2)	102	
	C(3)−H(3)···π	2.53		155	
2, form 2	C(10)−H(10)···O(2)	2.56	3.446(9)	137	70.3
	C(4)−H(4)···O(2)(intra)	2.45	2.875(9)	102	
2, form 3	C(16)−H(16)···O(2)	2.47	3.280(3)	140	62.4
	C(6)−H(6)···O(2)(intra)	2.52	2.913(2)	100	
2·CH_2Cl_2	N(1)−H(1)···O(1)	1.99	2.971(3)	162	60.3
	C(11)−H(11)···O(2)	2.43	3.359(4)	143	
3	N(1)−H(1)···O(1)	2.04	3.009(3)	160	62.6
	C(4)−H(4)···O(1)(intra)	2.48	2.902(4)	102	
4	N(1)−H(1)···O(1)	2.09	3.011(2)	151	66.5
	C(11)−H(11)···O(2)	2.36	3.335(3)	149	
	C(6)−H(6)···O(2)(intra)	2.50	2.900(2)	100	
5	N(1)−H(1)···O(1)	1.98	2.948(2)	160	64.9
	C(11)−H(11)···O(2)	2.46	3.535(1)	173	
	C(16)−H(16)···O(2)	2.40	3.248(2)	134	
	C(6)−H(6)···Cl(2)	2.73	3.457(2)	124	
	C(6)−H(6)···O(2)(intra)	2.48	2.895(2)	101	
	C(18)−Cl(2)···Cl(2)−C(18)	-	3.375(1)	142	
5·PhH	N(1)−H(1)···O(1)	2.03	3.006(3)	162	59.9
	C(11)−H(11)···O(2)	2.47	3.356(3)	139	
6	N(1)−H(1)···O(1)	1.97	2.937(2)	161	65.8
	C(6)−H(6)···O(1)	2.47	3.455(3)	151	
	C(10)−H(10)···O(2)	2.48	3.320(2)	134	
	C(17)−H(17)···O(2)	2.46	3.536(3)	175	
	C(4)−H(4)···O(2)(intra)	2.48	2.899(2)	101	
6·PhH	N(1)−H(1)···O(1)	2.07	3.025(4)	157	60.2
	C(19)−H(19)···O(2)	2.43	3.333(5)	140	

[a] Neutron-normalized values.

transient phase 2 under different experimental conditions, such as solvents of crystallization, new glassware, and change to another laboratory. Form 2 belongs to the anecdotal category of disappearing polymorphs.[24] Interconversion and stability of forms 1−3 was examined by differential scanning calorimetry (Figure 6). Form 1 melts at 142−143 °C, and the minor endotherm at 159 °C is assigned to concomitantly grown form 3. Form 2 undergoes phase transition at ∼140 °C followed by melting at 157−158 °C. Form 3 has a flat baseline and melts in a clear endotherm at 159−160 °C with no evidence of any other phase change. Melting point of form 3 is higher than that of form 1 by 17 °C. These thermal transformations and melting phenomenon were visualized in hot stage microscopy (Figure 7).

Phase transition of form 2 to 3 upon heating may be understood from their crystal packing diagrams. Tolyl rings of a cluster of four molecules are arranged in a herringbone T-motif in both crystal structures (Figures 2 and 3). These interdigitating tolyl groups are farther apart in form 2 and move closer in the crystal lattice of 3 with a decrease in inter-ring distance and *c*-axis (Figure 4). A C−H···O interaction of 2.47 Å in form 3 is longer in form 2 (2.56 Å, Table 2). The similarity between the monoclinic unit cells of crystal structures 2 and 3 is shown in Figure S2 (Supporting Information). Their cell edges follow a simple numerical relation: $a_{form3} \approx b_{form2}$ (8.29, 8.04 Å); $b_{form3} \approx a_{form2}$ (39.76, 42.04 Å); $c_{form3} \approx 0.5 \times c_{form2}$ (5.93, 12.34 Å). A molecular reorganization pathway for metastable form 2 to thermodynamic form 3 is suggested, but it is difficult to imagine a mechanism for the transformation of form 1 to 3 because their H bonding, molecular arrangement, and crystal structures are very different. We did not observe transformation of form 1 to 3 in thermal microscopy.

Crystal energies were estimated by calculating the lattice energy (U_{latt}) in Cerius[2] using a COMPASS force field, and the molecular conformation energy (E_{conf}) was computed in Gaussian 03 at the B3LYP/6-31G(d,p) level.[25] Energy values in Table 3 are consistent with the observed kinetic, metastable, and thermodynamic state of polymorphs 1−3. The sulfonamide molecule is flexible and has different torsion angles in the benzophenone and tosyl portions of the molecule (Figure 5). Energy differences between molecular conformers and crystal lattice energy are of comparable magnitude (a few kcal mol^{-1}, ΔE_{conf} and ΔU_{latt} columns in Table 3), and so their cumulative effect must be considered to compute total crystal energies (E_{total}).[22b] The necessity of taking molecular conformer stabilization (or destabilization) into account for computing crystal energy is underscored by the fact that ΔE_{total} rankings match with thermal measurements and phase relation but not the ΔU_{latt} order. Form 3 is the most stable polymorph (thermodynamic), form 1 is higher in energy by 2.54 kcal mol^{-1} (kinetic), and form 2 has very high relative energy of 7.86 kcal mol^{-1} (metastable, disappeared) based on ΔE_{total}. The energy difference of ∼2.5 kcal mol^{-1} between forms 1 and 3 is typical for polymorphs. The reason for the disappearing and metastable nature of crystal form 2 is its high-energy conformer in the crystal lattice. ΔU_{latt} energies do not agree with experimental data.

The major variation in conformers of **2** (as well as other derivatives discussed next) occurs in the N−N−S−C_{phenyl} moiety ($\tau_1 = 60-70°$); variation in N−N−C−C_{phenyl} torsions is minimal ($\Delta\tau_2$, $\Delta\tau_3$ <4°) with respect to the global minimum rotamer. The conformer energy vs torsion angle profile of **2** was therefore plotted by varying τ_1 while τ_2 and τ_3 were held constant (Figure 8). Simultaneous phenyl ring rotations to give several rotamers were not considered because for reasons of computational complexity. Moreover, this study is concerned with aryl group orientation around the SO_2NH functional group. Molecular conformations in observed polymorphs of **2** (Table 2) lie close to the global minimum rotamer at $\tau_1 = 60°$, within 10° torsion angle and 5 kcal mol^{-1} energy range. The energy

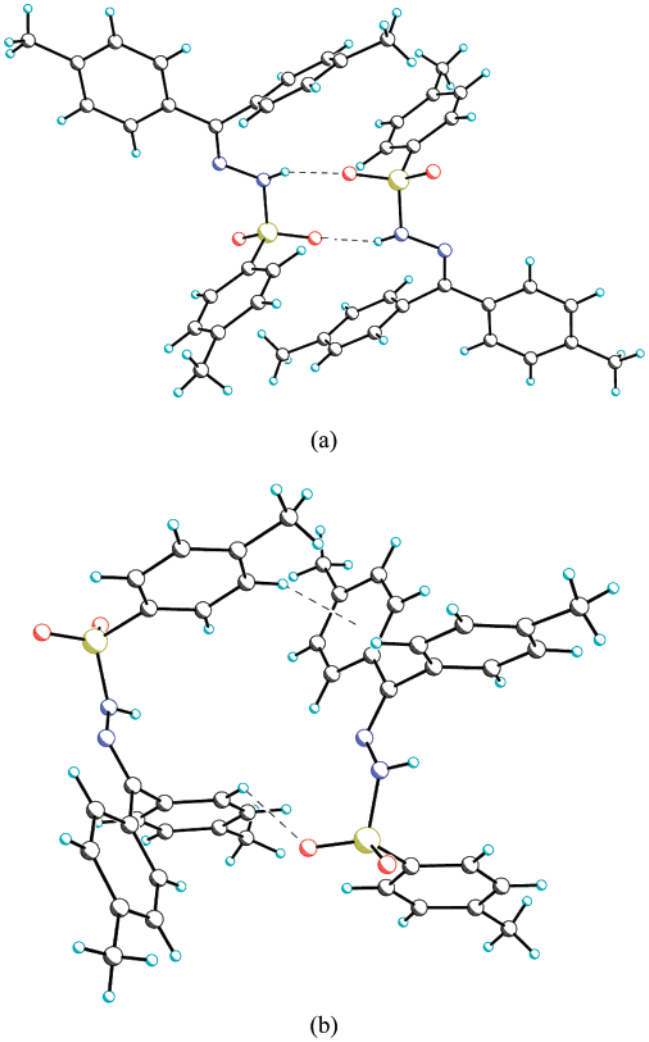

Figure 1. (a) Sulfonamide N−H···O dimer synthon of $R_2^2(8)$ graph set in the crystal structure of form 1 (*C*2/*c*) of molecule **2**. (b) Auxiliary C−H···O and C−H···π interactions from phenyl CH donors.

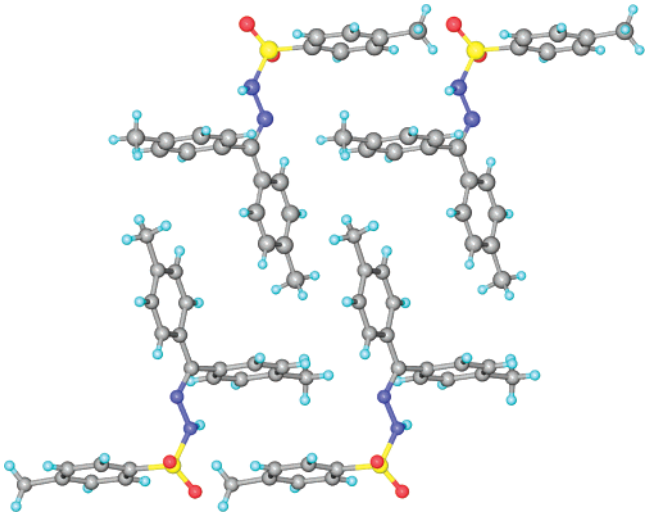

Figure 2. Sulfonamide NH donor not participating in N−H···O hydrogen bond or weak N−H···π interaction in form 2 (*C*2/*c*).

penalty of this value can be easily compensated by crystal structure stabilization due to stronger hydrogen bonds and better close packing. The significant torsion angle (τ_1) in form 1 of tolyl compound **2** is similar to monoclinic form II of acetone

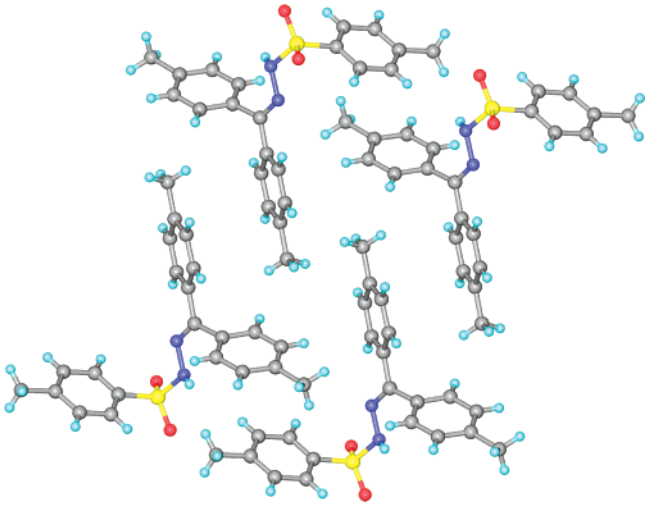

Figure 3. Sulfonamide NH donor not participating in conventional hydrogen bond or N−H···π interaction in form 3 ($P2_1/c$). Note the herringbone T-motif between tolyl groups.

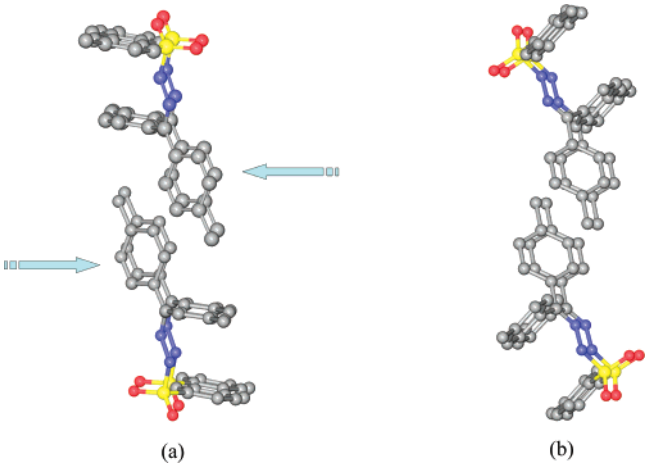

Figure 4. Movement of form 2 molecules toward each other (arrows in a) resulting in better eclipsing and more efficient close packing, as shown for dense form 3 (b). The intercentroid ring separation between tolyl rings decreases from 6.2 to 4.9 Å, and the *c*-axis contracts from 12.34 Å (*C*2/*c*, $Z = 8$) to 5.93 Å ($P2_1/c$, $Z = 4$). See Figure S2 for orientation of unit cell with respect to the molecular cluster.

hydrazone **1** (65.9, 64.5°, respectively), and these phenylogue-related crystal structures contain N−H···O═S dimer synthon anticipated at the beginning of this study (Scheme 2). However, the occurrence of non-H-bonded polymorphs in **2** came as a surprise.

Why does molecule **2** not make strong H bonds in its stable polymorph despite the SO_2NH group? The sulfonamide NH donor is not involved in conventional H bonding with an O/N/X^- acceptor in only 28/1266 crystal structures (frequency data in Scheme 3; see Figure S3 for molecular diagrams). A summary of the structural analysis of 28 sulfonamides in the CSD with no strong H bonds is as follows: (1) They are all secondary amides. (2) The C atom on NH group side is secondary/tertiary in several cases. (3) The absence of strong H bonding from the NH donor is not necessarily due to a deficiency of acceptor groups because some of these molecules have additional O/N acceptors (e.g., refcodes AYEQEA, AYEQIE, IHEJEK, SIZLUI). Steric crowding around the donor NH will weaken H-bonding ability, but this in itself is not sufficient to explain absence of H-bonding in forms 2 and 3. There are several N-*sec* and even N-*tert* sulfonamides with normal N−H···O H bonds

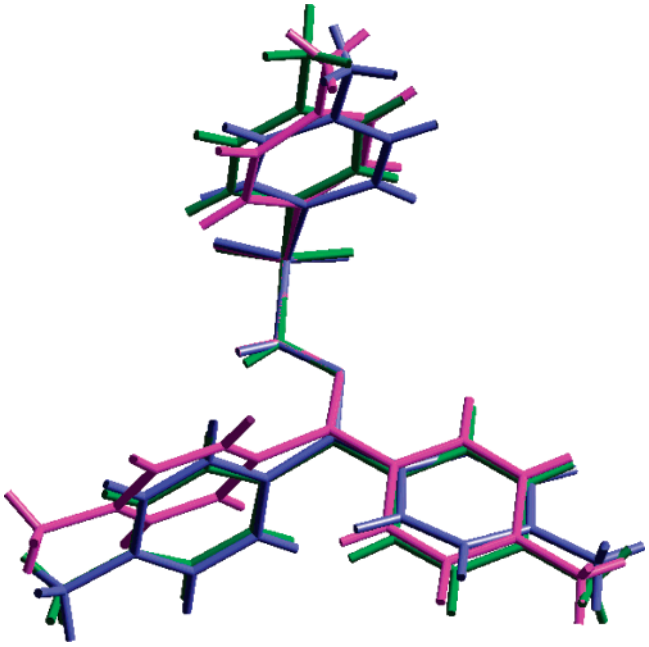

Figure 5. Molecular conformations of sulfonamide **2** in polymorphs 1−3 colored magenta = form 1, green = form 2, and blue = form 3. Tolyl groups are oriented differently in these three conformational polymorphs.

of 2.0−2.2 Å in the subdatabase of 1266 crystal structures (e.g., CSD refcodes ATAMOX, PELZOV, VOTZOT, PSAHPP, TIDQUS, AXAGOV). Incidentally, sulfonamide **2** could have formed a catemer motif of comparable synthon probability to the dimer, but we have not crystallized such a polymorph.

We believe that the reason for the presence of H bonding, or lack of it, in different crystal forms of **2** is related to the molecular conformation. Our hypothesis is supported in crystal structure prediction (reproduction) frames computed using the rigid body method starting from the experimental conformation as the input[22b] (Cerius,[2] COMPASS).[25] The idea of keeping the conformation fixed during structure simulation and energy minimization was to compare several putative crystal structures built from a particular conformer. Crystal structures were predicted starting from experimental conformers 1−3 in six common space groups ($P2_1/c$, $P\bar{1}$, $C2/c$, $Pbca$, $P2_12_12_1$, and $P2_1$), which include the observed space groups. The 10 lowest energy structures were analyzed, and the most stable predicted frame in the observed space group was compared with the experimental crystal structure (Table 4). The starting molecular conformer appears to implant its signature in the crystal structure. Superposition of nearest-neighbor molecules in the experimental crystal structure and the lowest energy predicted frame (designated as no. 1) in the appropriate space group show good similarity and overlay for all three polymorphs of **2** (Figure 9). The next best energy frames (second, third, etc.) have higher lattice energy by as much as 2 kcal mol^{-1} in each case. To further ascertain that molecular conformation is important in giving stable H-bonded clusters, the energy of the N−H···O═S dimer was computed for rotamers of **2** in Spartan 04 (RHF/6-31G**):[25] conformer 1 = −10.59 kcal mol^{-1}; conformer 2 = +6.31 kcal mol^{-1}; conformer 3 = −6.99 kcal mol^{-1}. Thus, conformer 1 favors H-bonded dimer as the nucleating aggregate compared to conformer 3 whereas conformer 2 is highly disfavored. The increasingly destabilizing nature of the H-bond dimer structures for conformers 3 and 2 was also revealed in polymorph predictor frames.[26] There is no low-energy H-bond dimer structure predicted for conformer 2 up to 5 kcal mol^{-1}, and dimer type structures of conformer 3 are ∼4 kcal mol^{-1} higher in energy than the minimized close packed structure listed in Table 4. Selecting the right molecular conformation in predicting the correct crystal structure of a conformationally flexible molecule is an important step.[22b,27]

Curtin−Hammett Energy Profile. The above situation—namely, a metastable, kinetic form and another stable, thermodynamic polymorph, the metastable crystal arising from a stable conformer while the thermodynamic crystal arising from a metastable conformer, with strong H bonding favoring the kinetic crystal whereas close packing stabilizing the thermodynamic crystal and a rapid equilibrium between low energy conformers in solution—is reminiscent of the Curtin−Hammett principle.[28] Curtin[28a] and Hammett stated that the product distribution in a reaction does not depend on the energy of the products but on how fast they form. Second, if a fast preequilibrium of conformers precedes a high-energy step, then the product distribution does not depend on the relative amounts of conformations in solution but on the activation energy required to form the product. The chemical events from molecular conformers to polymorphs 1 and 3 are depicted in the free energy vs crystallization pathway (Figure 10). The analogy to Curtin−Hammett-like reaction kinetics is justified because kinetic factors are deemed to be important in the crystallization of polymorphs.[10,11] Computed energy (differences) are approximated as free energy (differences) because the contribution of entropy is difficult to estimate. A solution of molecule **2** at near-ambient temperature ($\sim RT$ = 0.6 kcal mol^{-1} at 300 K) will have higher concentration of conformer 1 compared to conformers 3 and 2, in inverse relation to their ΔE_{conf} values (Table 3), along with several other low-lying conformations in dynamic equilibrium. The hydrogen-bonded crystal 1 will nucleate faster because there are more molecules in the required conformation and electrostatic stabilization of the H-bonded aggregate at long range (r^{-1}) will lower the $\Delta G_1^{\ddagger}$ barrier. On the other hand, there are fewer molecules of higher energy conformer 3 and weak van der Waals dispersive interactions operate only at short range (r^{-6}).[29] Thus, form 3 will nucleate slowly. The final crystal structure of form 3 is more stable than the H-bonded form 1 by 3.39 kcal mol^{-1} (ΔU_{latt}, Table 3) because the loss of H bond energy is more than compensated by dispersion energy in the latter, dense modification.

The Curtin−Hammett principle[28] has been invoked to explain reactivity in stereoselective reactions, asymmetric catalysis, enzyme catalysis, and photochemical transformations.[30] However, Curtin−Hammett reaction kinetics in the crystallization of conformational polymorphs and K/T relationships is not reported.[31] The present example of an H-bonded, kinetic form and a close-packed, thermodynamic polymorph illustrates two very different ways of crystal structure stabilization. Understanding the interplay of molecular conformation, H bonding and dense packing during self-assembly is a necessary step in understanding crystallization and polymorphism. It is quite likely that there are other polymorph clusters, known as well as new ones, which follow a similar pathway. Studies on the role of solvent (CH_2Cl_2/EtOH vs pure EtOH) in crystallization of polymorphs 1 and 3 will shed light on the nature of intermediates as crystallization progresses. For example, Davey[32] and coworkers showed by FT-IR spectroscopy that carboxylic acid dimer and catemer growth synthons in solution lead to the corresponding structural synthons in the solid state.

In addition to polymorphs **1**−**3**, we isolated a pseudopolymorph,[33] **2**·0.5CH_2Cl_2, from *n*-hexane/CH_2Cl_2 in the $P\bar{1}$ space

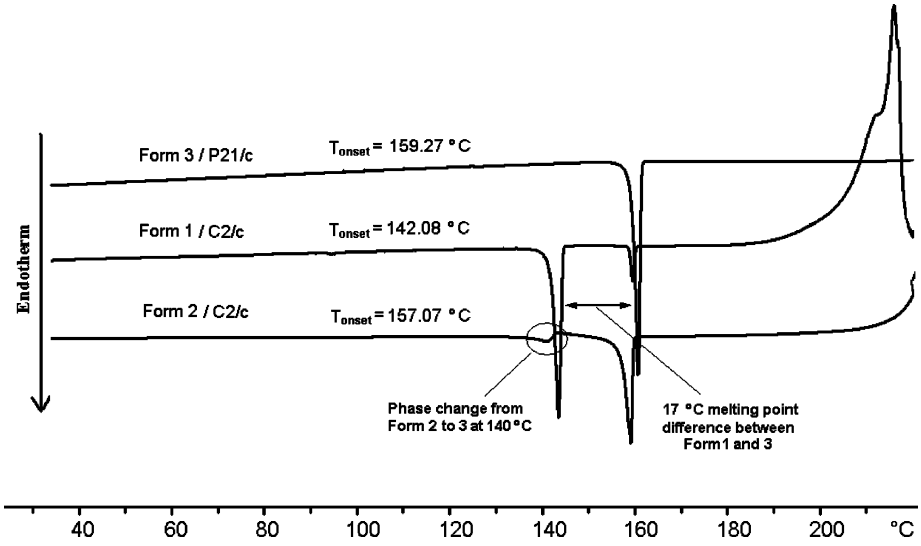

Figure 6. DSC of forms 1−3 of sulfonamide **2** polymorphs. Form 1 crystallized concomitantly with a minor amount of thermodynamic form 3. Form 2 undergoes phase transition to form 3 at 140 °C. Form 3 exhibits a sharp melting endotherm at 159 °C as the only phase transition.

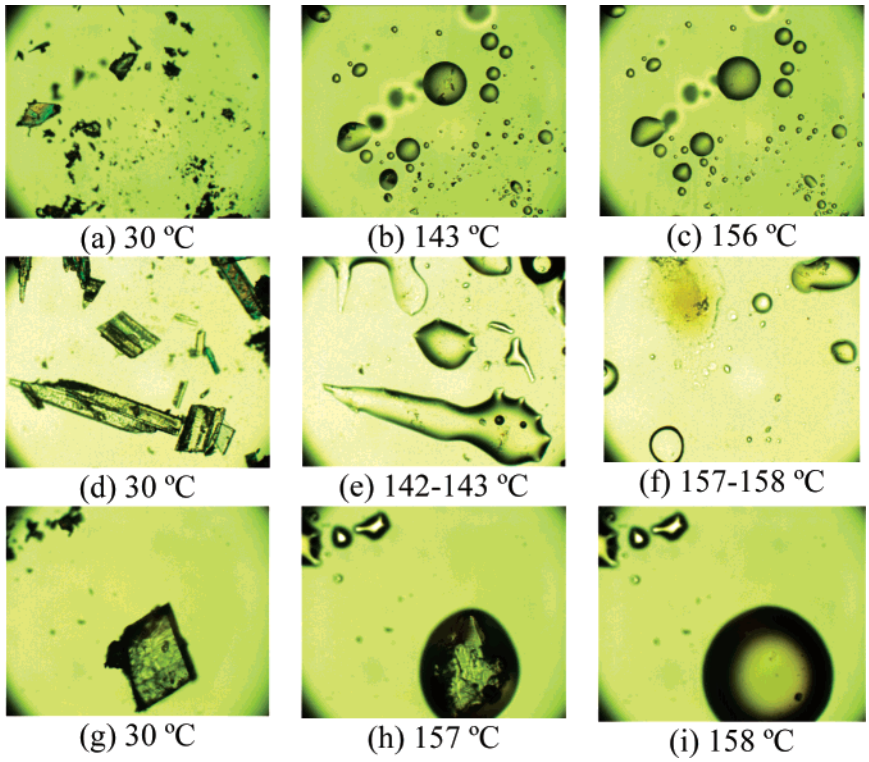

Figure 7. HSM frames. Form 1: As crystallized form 1 (a) melts at 142−143 °C, a few crystallites of concomitant form 3 melt at 156−157 °C. Form 2: As crystallized form 2 (d) melts at 142−143 °C (e) and form 3 (after phase transition) melts at 157−158 °C (f). Form 3: Pure form 3 (g) starts to melt at 157 °C (h), and this process completes at 158 °C (i). Sample was heated at 5 °C min^{-1}.

Table 3. Lattice Energy (U_{latt}, Cerius,[2] COMPASS, kcal mol^{-1}), Conformation Energy (E_{conf}, Gaussian 03, B3LYP/6-31G(d,p), kcal mol^{-1}), and Total Energy ($\Delta E_{total} = \Delta U_{latt} + \Delta E_{conf}$)

polymorph	U_{latt}	ΔU_{latt}	E_{conf}	ΔE_{conf}	ΔE_{total}
form 1	−41.13	3.39	−947 322.05	0.00	3.39
form 2	−42.10	2.42	−947 315.76	6.29[a]	8.71
form 3	−44.52	0.00	−947 321.20	0.85	0.85

[a] This value may be overestimated due to higher R-factor of 0.0724 for form 2.

group. Square channels of aromatic walls surround CH_2Cl_2 guest molecules in the hydrogen-bonded host structure of **2** (Figure 11). Solvent loss from **2**·0.5CH_2Cl_2 (Figure S4) at 105 °C in thermal gravimetry analysis is consistent with the host:guest stoichiometry. The higher melting endotherms at 141−143 and 158−160 °C are due to the unsolvated form 1 and stable form 3. The loss of solvent from the host:guest crystal gives the unsolvated dimer form 1. The minor endotherm corresponding to 3 could be due to the concomitantly growing stable phase in the bulk solid. We did not observe solid-to-solid transformation

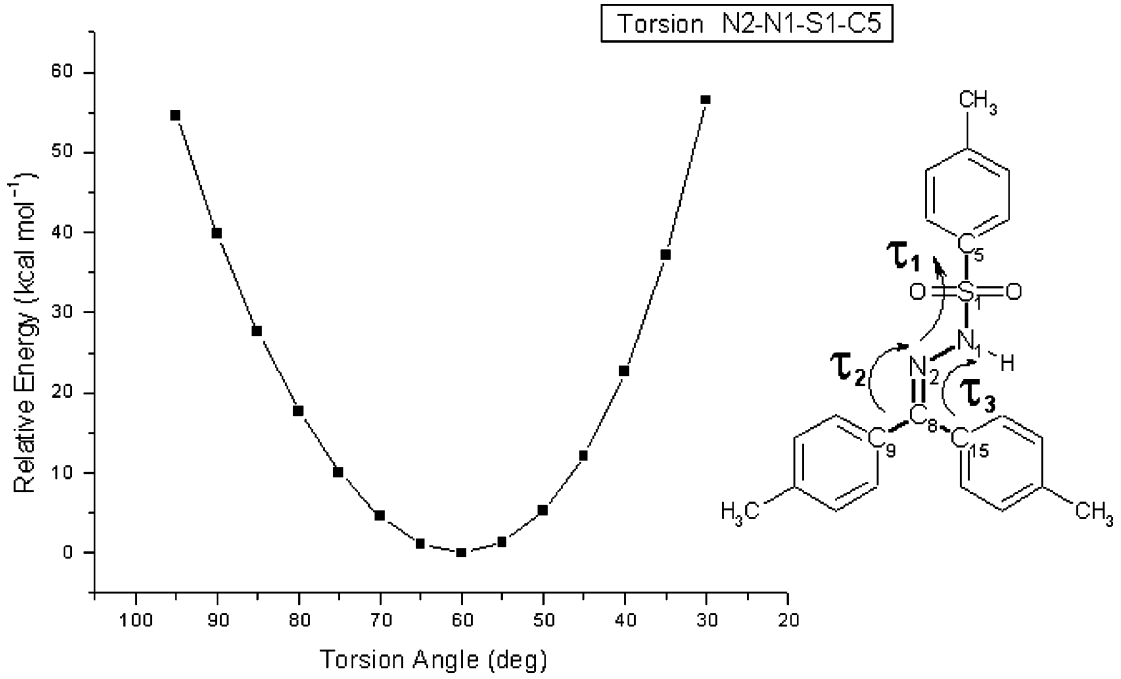

Figure 8. Potential energy surface map for molecule **2** showing the deep curvature near the stable SO_2NH torsion angle τ_1 = N2−N1−S1−C5 = 60°. Conformer energies were computed in Gaussian 03 and B3LYP/6-31G(d,p) and scaled to the lowest value = 0.0. The observed conformers (Table 2) are within a 10° torsion angle and 5 kcal mol^{-1} energy range of the stable conformation.

Table 4. Experimental Crystal Structures and Minimum Lattice Energy Structure Predicted Using Cerius[2] Polymorph Predictor in the Observed Space Group

polymorph	*a* (Å)	*b* (Å)	*c* (Å)	*β* (deg)	*V*/*Z* (Å^3)	U_{latt} (kcal mol^{-1})
			Form 1, *C*2/*c*			
frame no. 1[a] predicted	21.605	11.734	15.027	101.01	467.39	−41.13
form 1[b] expt min	21.609	11.734	15.029	101.01	467.56	−41.13
form 1 expt	22.009	11.976	15.185	100.94	491.25	
			Form 2, *C*2/*c*			
frame no. 1[a] predicted	42.327	7.846	11.874	108.63	467.05	−41.72
form 2[b] expt min	41.209	7.919	11.778	104.33	465.49	−42.10
form 2 expt	42.043	8.038	12.345	104.08	505.81	
			Form 3, $P2_1/c$			
frame no. 1[a] predicted	8.070	39.466	5.836	95.91	462.18	−42.77
form 3[b] expt min	8.144	38.986	5.764	95.49	455.47	−44.52
form 3 expt	8.297	39.758	5.935	97.29	485.50	

[a] Predicted structure in Cerius[2] (COMPASS force field, rigid body minimization). [b] Experimental crystal structure was minimized in Cerius.[2]

of forms 1 to 3 upon heating, but crystallization of minor amounts of thermodynamic form 3 from solution cannot be ruled out.

Analogues of 2. The *para*-methyl group on the benzophenone moiety of **2** was replaced with other groups, such as H, F, Cl, and Br (**3**−**6**). The iodo derivative **7** did not afford single crystals for X-ray diffraction. These compounds did not show any evidence of polymorphism under similar experimental protocols, such as crystallization from different solvents, solvent drop grinding, and using the ball-mill ground material as seeds. These structures are consistently stabilized by the sulfonamide N−H···O═S dimer (Figure 12 and Table 2). Chloro- and bromosulfonamides **5** and **6** crystallized as benzene solvates. Overlay of molecular conformers in these 10 crystal structures (Figure S5; 3 polymorphs of **2**, **3**−**6**, and 3 solvates) shows that there is considerable variation in the orientation of pendant aryl arms as well as phenyl ring rotamers. There is a degree of similarity expected when methyl group is exchanged with a halogen or among the halogen derivatives.[34] Form 1 of tolyl compound **2** and the chloro structure **5** are isomorphous and isostructural. Solvates **5**·0.5PhH and **6**·0.5PhH exhibit similar molecular packing in their isomorphous triclinic unit cells.

Phenyl−Tolyl Exchange. In this study, tolyl derivative **2** is trimorphic whereas phenyl compound **3** is not. In another system, we noted that 4,4-diphenyl-1,5-cyclohexadienone was tetramorphic[22] but not its tolyl derivative. The occurrence of polymorphism in phenyl/tolyl pairs of crystal structures was examined (Table 5). There are 119 tolyl-group-containing and 958 phenyl-containing organic polymorph hits, which represent 35 and 284 different polymorphic compounds, respectively. There are only 4 cases wherein polymorphs of both phenyl and tolyl compound pairs are reported. The exact reasons why tolyl sulfonamide **2** is trimorphic but phenyl compound **3** is not polymorphic are difficult to explain. *para*-substitution on the phenyl rings is too distant from the SO_2NH hydrogen-bonding region to pose serious steric problems for H bonding. The remote substitution change is unlikely to alter the inherent donor and acceptor strengths of the SO_2NH group. Yet there is no H bonding in two out of three polymorphs of **2** suggesting that the reason is perhaps specific to tolyl hydrazone. In the stable herringbone type packing of tolyl rings in form 3, which is also present in form 2, the tolyl−SO_2 and N−tolyl rings of neighboring molecules form a sandwich dimer (Figures 2 and 3). From packing considerations, this sandwich motif would be

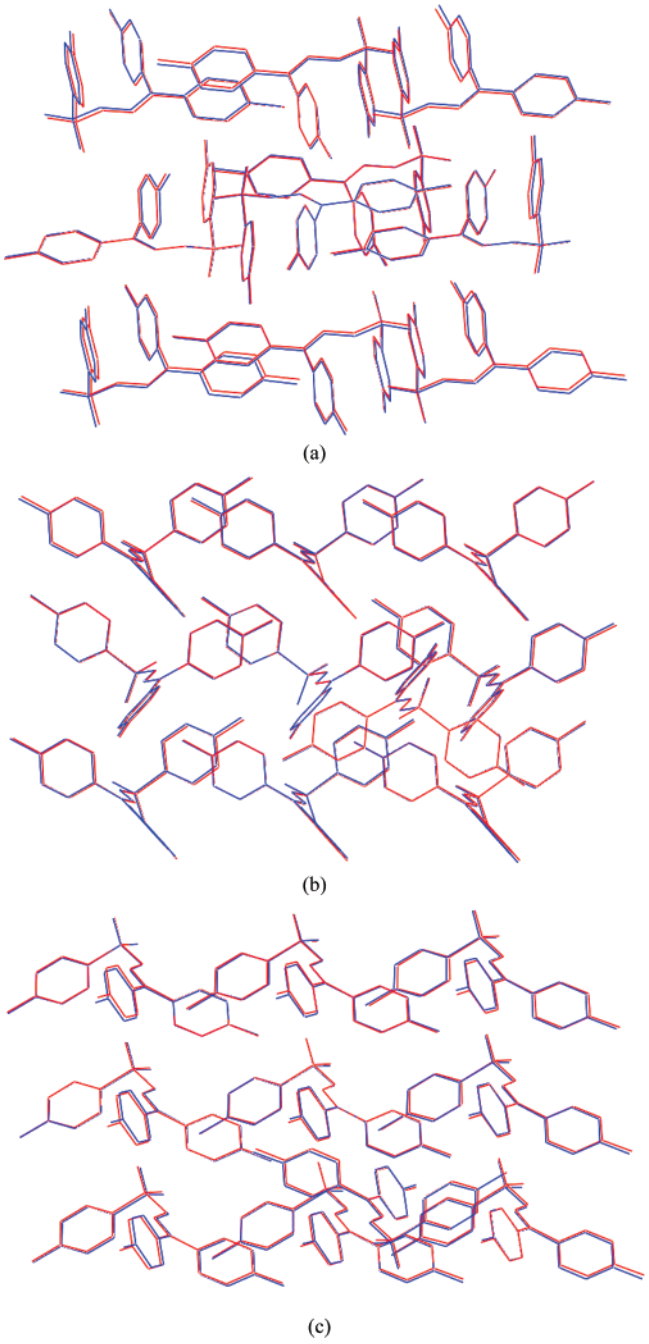

Figure 9. (a) Superposition of crystal form 1 and predicted frame no. 1 in *C*2/*c* space group. Rms deviation of 0.0019 indicates an excellent match of molecular clusters. (b) Superposition of crystal form 2 and predicted frame no. 1 in *C*2/*c* space group. Rms deviation of 0.0824 indicates a good match of molecular clusters. (c) Overlay of crystal form 3 and predicted frame no. 1 in $P2_1/c$ space group. Rms deviation of 0.1388 indicates a moderate match of molecular clusters. The 10 neighboring molecules were superposed in each case (red = experimental structure; blue = predicted structure).

stabilized when substituents on the two aryl groups are of similar size, i.e., for *N*-tolyl/*N*-(chlorophenyl). Indeed, the tolyl hydrazone of *p*-chlorophenyl sulfonamide is dimorphic,[35] with one of its crystal structures resembling form 1 of **2**.

Conclusions

The trimorph cluster of tolyl tosyl hydrazone **2** is a rare example of a molecule with SO_2NH functional group that exhibits H-bonded and non-H-bonded type synthon polymorphism. The hydrogen-bonded and close-packed crystal structures were assigned as kinetic and thermodynamic forms respectively from structural, thermochemical, and computational data. The presence of H bonding in one polymorph and its complete absence in another form provide experimental structures as reference to compare and calibrate calculated frames in crystal structure prediction programs. Even though several close-packed, dense structures are predicted near the global energy minimum, they are seldom realized experimentally. For pharmaceutical chemists, a stable, polymorph with no strong H bonds could mean a less bioavailable polymorph than an H-bonded drug. Such polymorphs offer the potential to formulate hydrophilic and hydrophobic forms of sulfa drugs. Crystallization of polymorphs 1 and 3 from interconverting molecular conformers is shown to follow the Curtin−Hammett energy profile in a supramolecular reaction.

Experimental Section

Synthesis and Crystallization. Bis(*p*-tolyl) ketone *p*-tosylhydrazone (**2**) and benzophenone derivative **3**−**6** were synthesized[36] as shown in Scheme 4.

To a stirred solution of *p*-toluenesulfonyl chloride (5.0 g, 26 mmol) in 30 mL of THF was added hydrazine hydrate (2.8 g, 55 mmol) dropwise at 0 °C. The reaction was continued for 30 min and the product extracted with ether to give *p*-toluenesulfonyl hydrazide (4.5 g, 90%). Mp: 108 °C.

Bis(*p*-tolyl) Ketone *p*-Tosylhydrazone (2). To a well-stirred solution of *p*-toluenesulfonyl hydrazide (1.2 g, 6.6 mmol) in 10 mL of ethanol was added an equimolar amount of 4,4′-dimethylbenzophenone (1.5 g, 6.6 mmol). The reaction mixture was refluxed for 2 h. Cooling the reaction mixture afforded crystalline bis(*p*-tolyl) ketone *p*-tosylhydrazone as precipitate. The solid was collected by filtration and washed with cold ethanol. Recrystallization from hot ethanol gave pure **2** (1.9 g, 75%). Mp: 159 °C. ^{1}H NMR (400 MHz, δ, $CDCl_3$): 2.33 (s, 3H), 2.42 (s, 6H), 6.97 (d, 8 Hz, 2H), 7.07 (d, 8 Hz, 2H), 7.28 (m, 6H), 7.50 (s, 1H), 7.82 (d, 8 Hz, 2H). IR (KBr): 3287, 3030, 1597, 1510, 1385, 1315, 1165 cm^{-1}. LC/MS (R_1 = 0.68): *m*/*z* 379, $(M + 1)^+$.

Benzophenone *p*-Tosylhydrazone (3). Mp: 180 °C. ^{1}H NMR (400 MHz, δ, $CDCl_3$): 2.52 (s, 3H), 7.21 (s, 2H), 7.34 (m, 11H), (s, 1H), 7.93 (d, 8 Hz, 2H). IR (KBr): 3202, 1595, 1491, 1444, 1377, 1168, 1055 cm^{-1}. LC/MS (R_1 = 0.69): *m*/*z* 351, $(M + 1)^+$.

Bis(*p*-flourophenyl) Ketone *p*-Tosylhydrazone (4). Mp: 164 °C. ^{1}H NMR (400 MHz, δ, $CDCl_3$): 2.44 (s, 3H), 6.96 (d, 8 Hz, 2H), 7.00 (m, 8H), 7.47 (s, 1H), 7.84 (d, 8 Hz, 2H). IR (KBr): 3177, 2762, 1599, 1508, 1381, 1332, 1226, 1157, 1068 cm^{-1}. LC/MS (R_1 = 0.69): *m*/*z* 387, $(M + 1)^+$.

Bis(*p*-chlorophenyl) Ketone *p*-Tosylhydrazone (5). Mp: 202 °C. ^{1}H NMR (400 MHz, δ, $CDCl_3$): 2.44 (s, 3H), 7.07 (d, 8 Hz, 2H), 7.25 (m, 6H), 7.48 (d, 8 Hz, 2H), 7.50 (d, 1H, 8 Hz), 7.83 (d, 8 Hz, 2H). IR (KBr): 3192, 1597, 1489, 1400, 1348, 1315, 1168, 1089, 1457 cm^{-1}. LC/MS (R_1 = 0.69): *m*/*z* 420, $(M + 1)^+$.

Bis(*p*-bromophenyl) Ketone *p*-Tosylhydrazone (6). Mp: 229 °C. ^{1}H NMR (400 MHz, δ, $CDCl_3$): 2.44 (s, 3H), 7.00 (d, 8 Hz, 2H), 7.26 (d, 10 Hz, 2H), 7.41(d, 10 Hz, 2H), 7.49(s, 1H), 7.67 (d, 8 Hz, 2H), 7.83 (d, 8 Hz, 2H). IR (KBr): 3190, 1597, 1489, 1394, 1340, 1167, 1068 cm^{-1}. LC/MS (R_1 = 0.69): *m*/*z* 509, $(M + 1)^+$.

Bis(*p*-iodophenyl) Ketone *p*-Tosylhydrazone (7). Mp: 201 °C (dec). ^{1}H NMR (400 MHz, δ, $CDCl_3$): 2.46 (s, 3H), 6.87 (d, 8 Hz, 2H), 7.14 (d, 10 Hz, 2H), 7.35 (d, 8 Hz, 2H), 7.50 (d, 1H), 7.64 (d, 8 Hz, 2H), 7.85 (m, 8 Hz, 4H). IR (KBr): 3246, 1579, 1367, 1170, 1033, 1008 cm^{-1}.

Crystallization of **2** from EtOH/CH_2Cl_2 at −5 °C gave platelike crystals of form 1 along with a few irregular blocks (Figure S6a). The plate morphology corresponds to form 1 as confirmed by unit cell checking. The irregular blocks are concomitantly growing form 3. There are also a few **2**·0.5CH_2Cl_2 solvate crystals (see next) in the same batch.

Grinding compound **2** with a few drops of CH_2Cl_2 added (kneading) and using the microcrystalline powder as seeds for crystallization from the same solvent at ambient temperature afforded very thin crystals of form 2 along with block crystals of form 3 (Figure S6b).

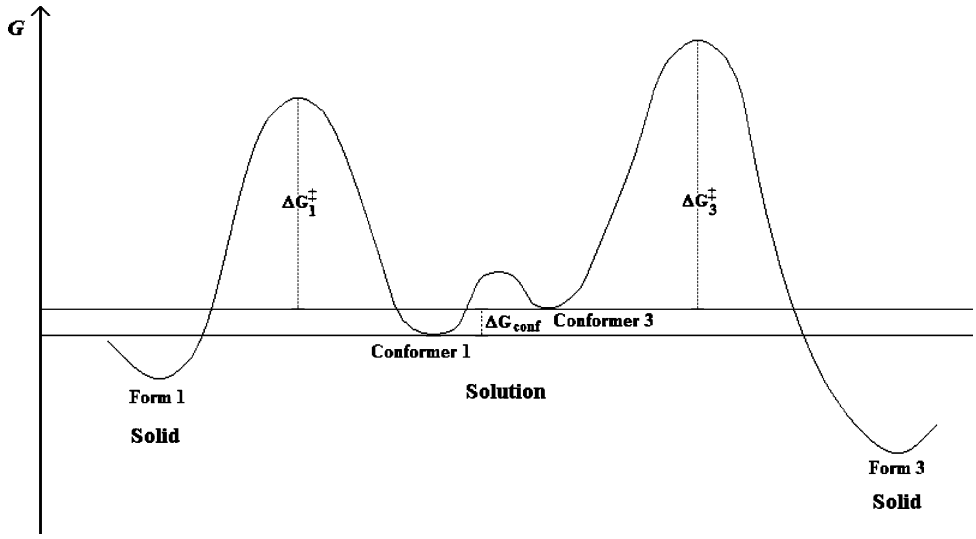

Figure 10. Curtin−Hammett principle in the crystallization of conformational polymorphs 1 and 3. Energy difference between conformers, $\Delta G_{conf} \sim 1-2$ kcal mol^{-1}, is less than the activation energy barrier for crystallization, $\Delta G^{\ddagger}$, which involves breaking of solute−solvent aggregates and formation of solute−solute nuclei. Free energy differences are estimated from computed conformer and lattice energies.

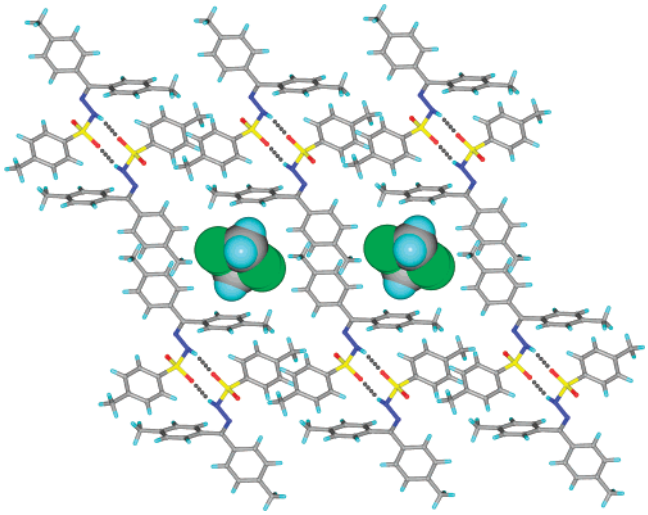

Figure 11. Sulfonamide N−H···O dimer synthon and CH_2Cl_2 molecules in the 8.8 × 7.1 Å voids created by tolyl groups in **2**·0.5CH_2Cl_2.

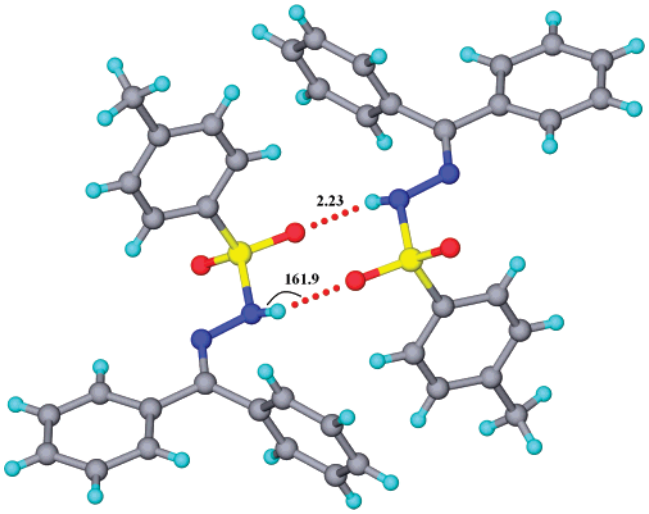

Figure 12. SO_2NH dimer synthon in phenyl derivate **3**. The distance and angle of N−H···O═S is indicated (Å, deg). Halogen derivatives **4**−**6** contain the same dimer synthon but show differences in crystal packing and space group.

Pure form 3 crystals of block and plate morphology crystallized by slow evaporation of a solution of compound **2** from EtOH at ambient temperature (Figure S6c).

Crystallization of **2** from CH_2Cl_2/*n*-hexane at ambient temperature gave platelike unstable crystals that became opaque within 1 day. Immediate data collection on a single crystal showed it as **2**·0.5CH_2Cl_2. The same solvated crystals were obtained concomitantly with form 1 also (unit cell check), but crystal quality is better by this method.

Crystallization of 3−6. Compound **3**−**5** were crystallized from the EtOH at ambient temperature. Compound **6** was crystallized from MeCN at ambient temperature. Iodo compound **7** did not afford single crystals or material suitable for powder XRD.

Solvates **5**·0.5PhH and **6**·0.5PhH crystallized from 1:1 EtOH/benzene mixture at ambient temperature.

X-ray Crystallography. Reflections were collected on Apex Bruker SMART CCD X-ray diffractometer. Crystal structures were solved using direct methods and refined by full-matrix least-squares refinement on F^2 with anisotropic displacement parameters for non-H atoms in SHELX-TL.[37] H atoms were refined isotropically except for N−H groups, which were located in the difference Fourier maps. The structure of twinned form 2 crystal was solved using CELL_NOW[38] (for p4p files) and TWINABS[39] (for *hkl* files). A new p4p file was created after thresholding the frames. This new p4p file when executed in CELL_NOW gave two different p4p files. The second file contains information about two orientation matrices. Data reduction were carried out in SAINT[40] using the second p4p file as input. Absorption correction was done by TWINABS to get two sets of *hkl* files, hkl4 and hkl5. Structure solution was carried out in XPREP by using hkl4 file, and refinement was executed on hkl5 file in SHELX-TL. Crystallographic parameters and final R-factors are acceptable for all structures.

Table 5. Occurrence of Polymorphism in Phenyl/Tolyl Crystal Structures in the CSD (Nov 2006 Update)

Tolyl Group Containing Polymorphic Structures = 119	
both tolyl and phenyl are polymorphic	4
tolyl is polymorphic but phenyl is not polymorphic	12
tolyl is polymorphic but phenyl structure is not reported	19
Phenyl Group Containing Polymorphic Structures = 958	
both phenyl and tolyl are polymorphic	2
phenyl is polymorphic but tolyl is not polymorphic	31
phenyl is polymorphic but tolyl structure is not reported	249

Refcodes of Four Phenyl−Tolyl Polymorph Pairs	
PHENOL CRESOL	UJIRIO EBIDUP
FEVNAV BPHENO	NEDZEB NEDYUQ

Gaussian 03, Spartan 04, and Cerius^2 Computations. Conformational energy (E_{conf}) of the three polymophs **2** was calculated using

Scheme 4. Compound 2 Prepared by the Condensation of *p*-Tosylhydrazine with Bis(*p*-tolyl) Ketone[a]

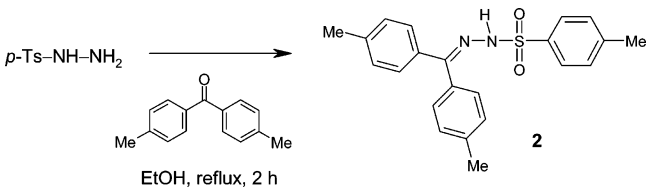

[a] Derivatives **3**−**7** were prepared in a similar manner.[36]

density functional theory (DFT) at the B3LYP/6-31G (d,p) level in Gaussian 03 using crystallographic coordinates as the input. Hydrogen atom positions were reoptimized keeping the heavy atoms fixed. The gas-phase rotamer of **2** was calculated, and a potential energy scan was carried out in 5° torsion angle intervals at the B3LYP/6-31G(d,p) level in Gaussian 03.

Lattice energies were computed for experimental polymorphs of **2** in the Cerius[2] program by energy minimization of crystal structures in COMPASS assigned with force field charges. COMPASS is better parametrized for structure prediction and energy minimization for a broad range of organic molecules. Crystal lattice energies are calibrated for the number of molecules in the unit cell (per molecule).

All simulations were carried out in version 4.8 of Cerius[2] molecular modeling environment running on a Silicon Graphics workstation. The crystal structure prediction of **2** was carried out in six common space groups ($P2_1$, $P2_1/c$, $C2/c$, $Pbca$, $P2_12_12_1$, $P\bar{1}$) using experimental conformers of three forms as the input. Atomic point charges were assigned in the COMPASS force field. Default options were used throughout with the fine search option in Monte Carlo simulation and for clustering of frames to get unique structures. Lattice energy minimization of predicted structures was carried out without any modifications except for the use of Ewald summation of van der Waals interactions at cutoff of 6.0 Å. All calculations were carried out by keeping the conformation fixed during minimization (rigid body method). The predicted frames (.res files) and crystal structures (.cif files) may be visualized in Mercury. Overlay diagrams in Figure 9 were created in COSET. These programs are developed and distributed by the CCDC.[13]

Hydrogen bond dimer energies for conformers 1−3 were calculated in Spartan 04 by extracting the dimer from the crystal structure of form 1 and minimizing its energy by keeping the heavy-atom positions fixed but optimizing H atom positions. Similarly, the energy of the dimer was calculated using molecular conformers 2 and 3 as the input. The energy of the molecule in each conformation was calculated independently in RHF 6-31G**.

Cambridge Structural Database Searches. Synthon Probability. The CSD (ConQuest 1.9, Nov 2006 update) was searched for sulfonamide compounds with the following qualifiers: organic; $R < 0.10$; 3-D coordinates determined; no errors; not polymeric. The subdatabase of 1266 hits was analyzed for hydrogen bond synthons shown in Scheme 3 in the following distance/angle range: H···A, 1.5−2.5 Å; D−H···A, 140−180°. Synthon probability is the number of hits containing a particular motif as a percentage of compounds that contain the required functional group (1266), as reported by Allen et al.[7a]

Polymorph Subdatabase. Polymorphs are those crystal structures having the qualifier polymorph, form, phase, or modification. Organic structures with R-factor <0.10 and 3-D coordinates determined were retrieved. The procedure is similar to a recent survey.[22b] This subset was searched for molecules containing the O−H or N−H group. Ionic, polymeric, disordered structures were excluded to make a subdatabase of 1868 hits. These structures were searched for the absence of strong O−H···O, O−H···N, N−H···O, and N−H···N hydrogen bonds (D−H···A) using the following contact criteria: H···A = 1.5−2.5 Å; D−H···A = 120−180°; D···A = 2.5−3.5 Å. The 93 polymorphic refcodes have no strong H bonds but contain OH/NH groups. These 93 clusters were manually analyzed to give 4 clusters such that one crystal structure has strong H bonds but the other form does not have H bonds. These four refcodes are KUVWON, MAMGUD, UCUGOP, and WEFKEY (Scheme 1).

Differential Scanning Calorimetry and Thermogravimetry. DSC was performed on a Mettler Toledo DSC 822e module, and TG, on a TGA/SDTA 851e module. Data were manipulated in the STAR software system. Samples were placed in crimped but vented aluminum pans for DSC (4−6 mg) and in open alumina cups for TG (8−12 mg). The temperature range was 30−250 °C at 2 °C min^{-1} for DSC and at 10 °C min^{-1} for TG. Samples were purged by a stream of dry N_2 flowing at 150 mL min^{-1} for DSC and 50 mL min^{-1} for TG.

Hot Stage Microscopy. HSM was performed on PolythermA hot stage and Heiztisch microscope supplied by Wagner & Munz. Moticam 1000 (1.3MP) camera supported by software Motic Image Plus 2.0ML was used to record images. About 1−2 mg of the sample was heated at 5 °C min^{-1} up to ∼200 °C.

Acknowledgment. We thank the DST for research funding (Grants SR/S5/OC-02/2002, SR/S1/RFOC-01/200) and for support of the CCD X-ray diffractometer (IRPHA) and the CMSD computational facility. The UPE program of UGC provided infrastructure funds at the UH. S.R. thanks the UGC for a fellowship.

Supporting Information Available: Table S1, Figures S1−S6 (PDF), crystallographic data (CIF), and predicted structure frames (RES). This material is available free of charge via the Internet at http://pubs.acs.org.

References

(1) (a) McCrone, W. C. In *Physics and Chemistry of the Organic Solid State*; Fox, D., Labes, M. M., Weissberger, A., Eds.; Wiley-Interscience: New York, 1965; Vol. 2, pp 725−767. (b) Bernstein, J. *Polymorphism in Molecular Crystals*; Clarendon: Oxford, U.K., 2002. (c) Hilfiker, R., Ed. *Polymorphism in the Pharmaceutical Industry*; Wiley-VCH: Weinheim, Germany, 2006. (d) Brittain, H. G. *J. Pharm. Sci.* **2007**, *96*, 705.

(2) (a) Groth, P. H. R. *Chemical Crystallography*; Engelmann: Leipzig, Germany, 1906−1919; Vols. 1−5. (b) Mitscherlich, E. *Abhl. Akad. Berlin* **1822**−**1823**, 43.

(3) (a) Kálmán, A.; Fábián, L.; Argay, G.; Bernath, G.; Gyarmati, Z. *J. Am. Chem. Soc.* **2003**, *125*, 34. (b) Weissbuch, I.; Torbeev, V. Y.; Leiserowitz Lahav, L. M. *Angew. Chem., Int. Ed.* **2005**, *44*, 3226. (c) Thallapally, P. K.; Jetti, R. K. R.; Katz, A. K.; Carrell, H. L.; Singh, K.; Lahiri, K.; Kotha, S.; Boese, R.; Desiraju, G. R. *Angew. Chem., Int. Ed.* **2004**, *43*, 1149. (d) David, W. I. F.; Shankland, K.; Pulham, C. R.; Bladgen, N.; Davey, R. J.; Song, M. *Angew. Chem., Int. Ed.* **2005**, *44*, 7032. (e) Vishweshwar, P.; McMahon, J. A.; Oliveira, M.; Peterson, M. L.; Zaworotko, M. J. *J. Am. Chem. Soc.* **2005**, *127*, 16802 (see also ref 3n). (f) Price, C. P.; Grzesiak, A. L.; Matzger, A. J. *J. Am. Chem. Soc.* **2005**, *127*, 5512. (g) Chen, S.; Guzei, I. A.; Yu, L. *J. Am. Chem. Soc.* **2005**, *127*, 9881. (h) Day, G. M.; Trask, A. V.; Motherwell, W. D. S.; Jones, W. *Chem. Commun.* **2006**, 54. (i) Guo, C.; Hickey, M. B.; Guggenheim, E. R.; Enkelmann, V.; Foxman, B. M. *Chem. Commun.* **2005**, 2220. (j) Rafilovich, M.; Bernstein, J. *J. Am. Chem. Soc.* **2006**, *128*, 12185. (k) Ahn, S.; Guo, F.; Kariuki, B. M.; Harris, K. D. M. *J. Am. Chem. Soc.* **2006**, *128*, 8441. (m) Roy, S.; Bhatt, P. M.; Nangia, A.; Kruger, G. J. *Cryst. Growth Des.* **2007**, *7*, 476. (n) Bond, A. D.; Boese, R.; Desiraju, G. R. *Angew. Chem., Int. Ed.* **2007**, *46*, 615.

(4) (a) Kitaigorodskii, A. I. *Organic Chemical Crystallography*; Consultants Bureau: New York, 1961. (b) Kitaigorodskii, A. I. *Molecular Crystals and Molecules*; Academic Press: New York, 1973.

(5) (a) Etter, M. C. *Acc. Chem. Res.* **1990**, *23*, 120. (b) Etter, M. C. *J. Phys. Chem.* **1991**, *95*, 4601.

(6) Desiraju, G. R. *Angew. Chem., Int. Ed. Engl.* **1995**, *34*, 2311.

(7) (a) Allen, F. H.; Motherwell, W. D. S.; Raithby, P. R.; Shields, G. P.; Taylor, R. *New. J. Chem.* **1999**, 25. (b) Chisholm, J.; Pidcock, E.; van de Streek, J.; Infantes, L.; Motherwell, S.; Allen, F. H. *CrystEngComm* **2006**, *8*, 11.

(8) Dunitz, J. D.; Gavezzotti, A. *Angew. Chem., Int. Ed.* **2005**, *44*, 1766.

(9) Desiraju, G. R. *CrystEngComm* **2002**, *4*, 499.

(10) (a) Jetti, R. K. R.; Boese, R.; Sarma, J. A. R. P.; Sreenivas Reddy, L.; Vishweshwar, P.; Desiraju, G. R. *Angew. Chem., Int. Ed.* **2003**, *42*, 1963. (b) Sarma, B.; Roy, S.; Nangia, A. *Chem. Commun.* **2006**, 4918. (c) Chew, J. W.; Black, S. N.; Chow, P. S.; Tan, R. B. H.; Carpenter, K. J. *CrystEngComm* **2007**, *9*, 128. (d) Rodríguez-Spong, B.; Price, C. P.; Jayashankar, A.; Matzger, A. J.; Rodríguez-Hornedo, N. *Adv. Drug. Delivery Rev.* **2004**, *56*, 241.

(11) Desiraju, G. R. *Nat. Mater.* **2002**, *1*, 77.

(12) Crystal structures and thermodynamic stability of organic polymorph clusters were compared in a seminal database study over a decade ago, but no examples of H-bonded vs non-H-bonded pairs were known at that time: Gavezzotti, A.; Fillippini, G. *J. Am. Chem. Soc*. **1995**, *117*, 12299.
(13) The Nov 2006 update of the CSD was searched (ConQuest) to extract data reported in this paper: www.ccdc.cam.ac.uk.
(14) (a) Weber, E.; Skobridis, K.; Wierig, A.; Nassimbeni, L. R.; Johnson, L. *J. Chem. Soc., Perkin Trans. 2* **1992**, 2123. (b) Senju, T.; Hoki, T.; Mizuguchi, J. *Acta Crystallogr*. **2005**, *E61*, o1061. (c) Senju, T.; Nishimura, N.; Hoki, T.; Mizuguchi, J. *Acta Crystallogr*. **2005**, *E61*, o2569. (d) Dias, H. V. R.; Singh, S. *J. Chem. Soc., Dalton Trans*. **2006**, 1995. (e) Bacchi, A.; Bosetti, E.; Carcelli, M.; Pelagatti, P.; Pelizzi, G.; Rogolino, D. *CrystEngComm* **2006**, 233.
(15) (a) Price, S. L. *CrystEngComm* **2004**, *6*, 344. (b) Lewis, T. C.; Tocher, D. A.; Price, S. L. *Cryst. Growth Des.* **2005**, *5*, 983.
(16) (a) Jeffrey, G. A. *An Introduction to Hydrogen Bonding*; Oxford University Press: New York, 1997. (b) Desiraju, G. R.; Steiner, T. *The Weak Hydrogen Bond in Structural Chemistry and Biology*; Oxford University Press: Oxford, U.K., 1999.
(17) Ojala, C. R.; Ojala, W. H.; Pennamon, S. Y.; Gleason, W. B. *Acta Crystallogr*. **1998**, C*54*, 57.
(18) Aitipamula, S.; Nangia, A. *Chem. Commun*. **2005**, 3159.
(19) Kálmán, A. *Acta Crystallogr*. **2005**, *B61*, 536.
(20) (a) Bryn, S. R.; Pfeiffer, R. R.; Stowell, J. G. *Solid-State Chemistry of Drugs*; SSCI: West Lafayette, IN, 1999. (b) Blagden, N.; Davey, R. J.; Lieberman, H. F.; Williams, L.; Payne, R.; Roberts, R.; Rowe, R.; Docherty, R. *J. Chem. Soc., Faraday Trans.* **1998**, *94*, 1035. (c) Hughes, D. S.; Hursthouse, M. B.; Lancaster, R. W.; Tavener, S.; Threlfall, T. L. *Chem. Commun.* **2001**, 603.
(21) Bernstein, J.; Davis, R. E.; Shimoni, L.; Chang, N.-L. *Angew. Chem., Int. Ed. Engl*. **1995**, *34*, 1555.
(22) (a) Kumar, V. S. S.; Addlagatta, A.; Nangia, A.; Robinson, W. T.; Broder, C. K. R.; Mondal, R.; Evans, I. R.; Howard, J. A. K.; Allen, F. H. *Angew. Chem., Int. Ed.* **2002**, *41*, 3848. (b) Roy, S.; Banerjee, R.; Nangia, A.; Kruger, G. J. *Chem.*—Eur. J. **2006**, *12*, 3777.
(23) (a) Trask, A. V.; Hanes, D. A.; Motherwell, W. D. S.; Jones, W. *Chem. Commun*. **2006**, 51. (b) Braga, D.; Grepioni, F. *Angew. Chem., Int. Ed*. **2004**, *43*, 4002.
(24) (a) Dunitz, J. D.; Bernstein, J. *Acc. Chem. Res*. **1995**, *28*, 193. (b) Henck, J.-O.; Bernstein, J.; Ellern, A.; Boese, R. *J. Am. Chem. Soc.* **2001**, *123*, 1834. (c) Bombicz, P.; Czugler, M.; Tellgren, R.; Kálmán, A. *Angew. Chem., Int. Ed*. **2003**, *42*, 1957.
(25) (a) Cerius^2 suite of software for crystal lattice energy calculation and crystal structure prediction: www.accelrys.com. (b) Gaussian 03 package for ab initio calculation of molecule energy, revision B.05: www.gaussian.com. (c) Spartan 04 to calculate hydrogen bond energy of dimers: www.wavefun.com. See details on energy calculations and structure prediction in a previous paper.[22b]
(26) Full details of crystal structure prediction and rankings in rigid and flexible body computations will be reported shortly.
(27) Nowell, H.; Price, S. L. *Acta Crystallogr*. **2005**, *B61*, 558 and references therein.
(28) (a) Curtin, D. Y. *Rec. Chem. Prog*. **1954**, *15*, 111. (b) Seeman, J. L. *Chem. Rev*. **1983**, *83*, 83. (c) Carey, F. A.; Sandberg, R. J. *Advanced Organic Chemistry, Part A-Structure and Mechanisms*, 4th ed.; Plenum Press: New York, 2006; pp 220−222.
(29) Desiraju, G. R. *Acc. Chem. Res.* **2002**, *35*, 565.
(30) (a) Xia, W.; Scheffer, J. R.; Patrick, B. O. *CrystEngComm* **2005**, *7*, 728. (b) Howell, S. J.; Ashton, P. R.; Spencer, N.; Philp, D. *Org. Lett.* **2001**, *3*, 353. (c) Lodola, A.; Mor, M.; Zurek, J.; Tarzia, G.; Piomelli, D.; Harvey, J. N.; Milholland, A. J. *Biophys. J.* **2007**, *92*, L20.
(31) A search of scholar.google.com for keywords Curtin, Hammett, and Polymorph gave only two hits—refs 10a and 11. Besides the statement that "the Curtin−Hammett principle can operate in crystallization, leading to polymorphism.",[10a] there is no discussion on the crystallization of polymorphs and the Curtin−Hammett principle.
(32) Davey, R. J.; Dent, G.; Mughal, R. K.; Praveen, S. *Cryst. Growth Des.* **2006**, *6*, 1788.
(33) (a) Nangia, A.; Desiraju, G. R. *Chem. Commun.* **1999**, 605. (b) Mondal, R.; Howard, J. A. K. *CrystEngComm* **2005**, *7*, 462.
(34) (a) Muthuraman, M.; Fur, Y. L.; Bagieu-Beucher, M.; Masse, R.; Nicoud, J.-F.; George, S.; Nangia, A.; Desiraju, G. R. *J. Solid State Chem*. **2000**, *152*, 221. (b) Saha, B. K.; Nangia, A.; Nicoud, J.-F. *Cryst. Growth Des.* **2006**, *6*, 1278. (c) Saha, B. K.; Nangia, A. *Cryst. Growth Des.* **2007**, *7*, 393.
(35) Unpublished results.
(36) (a) Friedman, L.; Litle, R. L.; Reichle, W. R. *Organic Syntheses*; Wiley and Sons: New York, 1973; Collect. Vol. V, p 1055. (b) Miller, V. P.; Yang, D.; Weigel, T. M.; Han, O.; Liu, H. *J. Org. Chem*. **1989**, *54*, 4175.
(37) (a) *SMART (version 5.625) and SHELX-TL (version 6.12)*; Bruker AXS Inc.: Madison, WI, 2000. (b) Sheldrick, G. M. *SHELXS-97 and SHELXL-97*; University of Göttingen: Göttingen, Germany, 1997.
(38) Sheldrick, G. M. *CELL_NOW*; University of Göttingen: Göttingen, Germany, 2004.
(39) Sheldrick, G. M. *TWINABS*, version 1.05; University of Göttingen: Göttingen, Germany, 2003.
(40) *SAINT-Plus*, version 6.45; Bruker AXS Inc.: Madison, WI, 2003.

CG070542T